

# *Hydrogen sulfide regulates hippocampal neuron excitability via S-sulfhydration of Kv2.1*

Article

Published Version

Creative Commons: Attribution 4.0 (CC-BY)

Open Access

Dallas, M. L. ORCID: <https://orcid.org/0000-0002-5190-0522>, Al-Owais, M. M., Hettiarachchi, N. T., Vandiver, M. S., Jarosz-Griffiths, H. H., Scragg, J. L., Boyle, J. P., Dallas, D. and Peers, C. (2021) Hydrogen sulfide regulates hippocampal neuron excitability via S-sulfhydration of Kv2.1. Scientific Reports, 11. 8194. ISSN 2045-2322 doi: <https://doi.org/10.1038/s41598-021-87646-5> Available at <https://centaur.reading.ac.uk/97442/>

It is advisable to refer to the publisher's version if you intend to cite from the work. See [Guidance on citing](#).

Published version at: <https://doi.org/10.1038/s41598-021-87646-5>

To link to this article DOI: <http://dx.doi.org/10.1038/s41598-021-87646-5>

Publisher: Nature Publishing Group

All outputs in CentAUR are protected by Intellectual Property Rights law, including copyright law. Copyright and IPR is retained by the creators or other copyright holders. Terms and conditions for use of this material are defined in the [End User Agreement](#).

[www.reading.ac.uk/centaur](http://www.reading.ac.uk/centaur)

**CentAUR**

Central Archive at the University of Reading

Reading's research outputs online



OPEN

# Hydrogen sulfide regulates hippocampal neuron excitability via S-sulfhydration of Kv2.1

Mark L. Dallas<sup>1</sup> , Moza M. Al-Owais<sup>2,5</sup> , Nishani T. Hettiarachchi<sup>2</sup>, Matthew Scott Vandiver<sup>3</sup>, Heledd H. Jarosz-Griffiths<sup>4</sup>, Jason L. Scragg<sup>2</sup>, John P. Boyle<sup>2</sup>, Derek Steele<sup>5</sup> & Chris Peers<sup>1,6</sup>

Hydrogen sulfide (H<sub>2</sub>S) is gaining interest as a mammalian signalling molecule with wide ranging effects. S-sulfhydration is one mechanism that is emerging as a key post translational modification through which H<sub>2</sub>S acts. Ion channels and neuronal receptors are key target proteins for S-sulfhydration and this can influence a range of neuronal functions. Voltage-gated K<sup>+</sup> channels, including Kv2.1, are fundamental components of neuronal excitability. Here, we show that both recombinant and native rat Kv2.1 channels are inhibited by the H<sub>2</sub>S donors, NaHS and GYY4137. Biochemical investigations revealed that NaHS treatment leads to S-sulfhydration of the full length wild type Kv2.1 protein which was absent (as was functional regulation by H<sub>2</sub>S) in the C73A mutant form of the channel. Functional experiments utilising primary rat hippocampal neurons indicated that NaHS augments action potential firing and thereby increases neuronal excitability. These studies highlight an important role for H<sub>2</sub>S in shaping cellular excitability through S-sulfhydration of Kv2.1 at C73 within the central nervous system.

Current awareness of the biological roles of endogenous hydrogen sulfide (H<sub>2</sub>S) is expanding rapidly, as our understanding of its production and cellular targets continue to develop<sup>1–3</sup>. Enzymatic production of H<sub>2</sub>S from cysteine is regulated by cystathionine γ lyase (CSE) and cystathionine β synthetase (CBS). With reference to the central nervous system (CNS) 3-mercaptopyruvate sulfurtransferase (3MST) along with cysteine aminotransferase has also been demonstrated to generate H<sub>2</sub>S in the brain<sup>4,5</sup>, with additional H<sub>2</sub>S protein-bound sulphur “stores”<sup>6</sup>. H<sub>2</sub>S levels in the brain have been reported in the μM range<sup>7,8</sup>, however real time measurements are challenging given the physiochemical nature of the gasotransmitter<sup>9–11</sup>. While physiological levels are known to mediate diverse signalling cascades, there is the potential to develop cellular toxicity however a consensus on the molecular basis of H<sub>2</sub>S mediated neurotoxicity is lacking<sup>12,13</sup>. Furthermore, some effects of H<sub>2</sub>S have been demonstrated to occur through polysulfides (H<sub>2</sub>S<sub>n</sub>) which are important physiological signalling species in themselves<sup>14,15</sup>.

In the CNS, the gasotransmitter, H<sub>2</sub>S promotes induction of long-term potentiation<sup>7</sup>, modifies astrocytic Ca<sup>2+</sup> signalling<sup>16</sup> and protects neurons against oxidative stress<sup>17</sup>. Given the diversity of effects, it is perhaps surprising that one mechanism of action is emerging as vital in regulating these processes; the modification of protein thiol groups termed S-sulfhydration, in which the thiol –SH groups in cysteine residues are converted to persulfide –SSH groups<sup>1,18</sup>, leading to modulation of protein function and/or protection against oxidation. Such a post-translational modification is analogous to the widespread S-nitrosylation of diverse proteins by nitric oxide<sup>19</sup>. Studies have suggested that up to 50% of cellular proteins may be basally S-sulfhydrated<sup>1,18</sup>, implying that this post-translational modification is of widespread physiological importance.

Ion channels are a significant and expanding family of substrates for regulation by H<sub>2</sub>S<sup>20</sup>. Clear evidence for modulation of vascular K<sub>ATP</sub> channels by S-sulfhydration has been presented<sup>21</sup> and, given the numerous ion channels within the CNS that may be modulated by H<sub>2</sub>S<sup>20</sup>, it seems likely (although has yet to be demonstrated) that S-sulfhydration may be an important modulatory mechanism within the CNS. Voltage-gated potassium channels (Kv) are the most diverse ion channel family<sup>22</sup> and some subfamilies have already been reported as

<sup>1</sup>Reading School of Pharmacy, University of Reading, Reading RG6 6UB, UK. <sup>2</sup>Division of Cardiovascular and Diabetes Research, LIGHT, Faculty of Medicine and Health, University of Leeds, Leeds LS2 9JT, UK. <sup>3</sup>Department of Neuroscience, Johns Hopkins University School of Medicine, Baltimore, USA. <sup>4</sup>Leeds Institute of Rheumatic and Musculoskeletal Medicine, University of Leeds, Leeds LS2 9JT, UK. <sup>5</sup>School of Biomedical Sciences, Faculty of Biological Sciences, University of Leeds, Leeds LS2 9JT, UK. <sup>6</sup>Chris Peers is deceased. ✉email: m.dallas@reading.ac.uk; m.al-owais@leeds.ac.uk

substrates for  $H_2S^{23,24}$ . In the present study, we have investigated the potential modulation of the delayed rectifier channel Kv2.1 by  $H_2S$ . This channel is unique in that it is regulated through post translational modifications that have profound functional consequences. For example, phosphorylation of Kv2.1 dramatically alters excitability of central neurons, as has been demonstrated in hippocampal neurons<sup>25–27</sup> suggesting that the mechanisms regulating these channels are highly important to signalling within the CNS.

## Experimental procedures

**HEK293 cell culture.** Wild-type and Kv2.1-transfected HEK293 cells (the latter a gift from Dr JS Trimmer, Davis, CA) were maintained at 37 °C (95% air:5%  $CO_2$ ) in DMEM containing 2mM glutamine, 10% fetal bovine serum, 1% Glutamax and 1% penicillin/streptomycin<sup>28</sup>. The Kv2.1 gene (*KCNB1*) was originally cloned from rat. The C29A, C73A and C831A mutations were introduced into WT rat Kv2.1 using the Quik-Change Site-Directed Mutagenesis Kit (Stratagene, Cheadle, UK) according to the manufacturer's instructions. All constructs were verified by DNA sequence analysis before transfection. Cells were plated either onto coverslips for electrophysiology or utilised for biochemical assays (see below).

**Primary neuron culture.** Preparation of rodent neuronal cultures was carried out in accordance with local University of Leeds regulations, and reported in line with ARRIVE guidelines. Procedures were approved by the local University of Leeds ethics committee. Briefly, hippocampi from 6 to 8 day old Wistar rats were removed for mechanical and enzymatic dissociation as described before<sup>28</sup>. Tissue was incubated (15 min at 37 °C) in phosphate buffered saline containing 0.25 µg/ml trypsin (EC 4.4.21.4, from bovine pancreas; Sigma). Trypsin digestion was terminated by the addition of an equal volume of buffer containing 16 µg/ml soy bean trypsin inhibitor (SBTI, type I-S; Sigma), 0.5 µg/ml DNaseI (EC 3.1.21.1 type II from bovine pancreas; 125 kU/ml; Sigma) and 1.5 mM  $MgSO_4$ . Following centrifugation (3000 rpm for 5 min), cells were resuspended in minimal Earle's medium (MEM) supplemented with 10% fetal calf serum, 19 mM KCl, 13 mM glucose, 50 IU/ml penicillin and 50 µg/ml streptomycin. 100 µl of cell suspension was plated onto 10 mm diameter poly-L-lysine coated coverslips in a 24-well plate for electrophysiology. After 24 h, this medium was replaced with one containing 10% horse serum (in place of fetal calf serum) and 80 µM fluorodexoyuridine (FUDR) to prevent the proliferation of non-neuronal cells. By 48 h, this medium was exchanged for one containing Neurobasal media, supplemented with 2% B-27, 1% penicillin/streptomycin, 0.5 mM L-glutamine and 25 µM L-glutamic acid. Cells were maintained in a humidified incubator at 37 °C (95% air: 5%  $CO_2$ ) for 7 days. All experiments were performed using cells cultured for 7 to 14 days.

**Electrophysiology.** Fragments of coverslip with attached cells were transferred to a perfused (3–5 ml/min) recording chamber mounted on the stage of an Olympus CK40 inverted microscope. As previously described<sup>28</sup>, the standard perfusate for HEK293 cells (pH 7.2,  $22 \pm 1$  °C) was composed of (in mM): NaCl (140), KCl (5),  $MgCl_2$  (2), HEPES (10),  $CaCl_2$  (2), and glucose (10). Patch pipettes had resistances 4–6 MΩ. Series resistance was monitored after breaking into the whole cell configuration throughout the duration of experiments. If a significant increase occurred (> 20%), the experiment was terminated. Series resistance was monitored and compensated for (60–80%) after breaking into the whole cell configuration throughout the duration of experiments. The pipette solution (pH 7.2) consisted of (in mM): KCl (140), EGTA (5),  $MgCl_2$  (2),  $CaCl_2$  (1), HEPES (10), and glucose (10). For some experiments an anti-Kv2.1 antibody (Neuromab, CA) was added to the intracellular solution (final concentration of 0.5 µg/ml). For HEK293 cells, two voltage protocols were adopted: (1) a series of depolarising steps from –100 to +80 mV in 10 mV increments for 500ms, (2) a single step to +50 mV from –70 mV for 100 ms at 0.2 Hz. For hippocampal neurons, similar protocols were used except for the inclusion of a single 30 ms prepulse to –50 mV, to inactivate 'A'-type potassium currents. Signals were sampled at 10 kHz and low pass filtered at 2 kHz. To investigate neuronal excitability, current-clamp recordings were undertaken. Action potential recordings were made in whole-cell current-clamp mode with signals low-pass filtered at 2 kHz and sampled at 10 kHz. Action potentials were evoked by 500 ms current pulses (0–200 pA). The perfusate consisted of (in mM): NaCl (135), KCl (5),  $CaCl_2$  (2.5),  $MgCl_2$  (1.2), HEPES (5), and glucose (10), and was bubbled with mixed gas (95% air/5%  $CO_2$ ; pH 7.4). Intracellular solution (pH 7.2) consisted of (in mM): Kgluconate (110), NaCl (10), EGTA (11),  $Na_2ATP$  (2),  $MgCl_2$  (2),  $CaCl_2$  (0.1),  $NaGTP$  (0.3), and HEPES (10). Voltage- and current-clamp analysis protocols were performed using an Axopatch 200A amplifier/Digidata 1200 interface controlled by Clampex 9.0 software (Molecular Devices, Foster City, CA). Offline analysis was performed using Clampfit 9.0 (Molecular Devices, Foster City, CA). Conductance values (G) were calculated as previously described<sup>27</sup>. Results are presented as means  $\pm$  S.E.M., and statistical analysis performed using unpaired Student's *t*-tests where  $P < 0.05$  was considered statistically significant.

**Modified biotin switch assay.** The assay was carried out as described previously<sup>18</sup> but with some modifications: HEK293 cells expressing Kv2.1 WT or C73A mutant were cultured at 37 °C in a humidified atmosphere containing 95% air and 5%  $CO_2$  and treated with 250 µM NaHS for 1 h or 2 h when 90% confluent. Untreated cells were used as a controls. Cells were homogenized in non-denaturing lysis buffer (Tris-HCl 50 mM; NaCl 300 mM; EDTA 5 mM; Triton X-100 1%) unless stated otherwise all buffers were supplemented with complete cocktail protease inhibitors tablets (Life Science Roche, UK). Lysate was collected via centrifugation at 13,000 g (10 min at 4 °C). Protein concentration was determined using Pierce BCA Protein Assay Kit (Thermo Fisher Scientific, UK) according to the manufacturer's instructions. To block free cysteines, lysates (250 µg total protein) were added to blocking buffer (HEPES 250 mM, pH 7.7; EDTA 1 mM plus 25% SDS and 20 mM methyl methanethiosulfonate [MMTS]) and incubated at 50 °C for 20 min with constant shaking at 1400 rpm. The samples were buffer exchanged and MMTS was removed using protein desalting spin columns (Thermo scientific,

UK). Biotin-*N*-[6-(biotinamido)hexyl]-3'-(2'-pyridyldithio) propionamide (HPDP) was added to the buffer exchanged protein samples to a final concentration of 4 mM and incubated in the dark for 90 min at room temperature with constant shaking (1400 rpm), biotinylated proteins were then buffer exchanged using spin columns to remove biotin-HPDP in the neutralization buffer (HEPES 20 mM; NaCl 100 mM; EDTA 1 mM Triton X-100 0.5%, pH 7.7) and precipitated by streptavidin-agarose beads, for 16 h at 4 °C. The biotinylated proteins were eluted by SDS-PAGE sample buffer and subjected to Western blot analysis.

Anti-Kv2.1 antibodies K89/34 (NeuroMab, Davis, CA) were used to detect Kv2.1 WT and C73A.  $\beta$ -Actin was used as loading control (Sigma-Aldrich, UK). ImageJ software (NIH, Bethesda, USA) was used to analyse band intensities for Kv2.1 before and after the assay.

**Hydrogen sulfide generation.** Hydrogen sulfide ( $H_2S$ ) was produced using the donor molecule sodium hydrosulfide (NaHS, Sigma-Aldrich, UK) and made up as a stock solution in Hank's Balanced Salt Solution. This stock was then diluted in the perfusate to give the working concentration as stated in the text. To avoid degradation and loss of  $H_2S$  the stocks were routinely made up immediately prior to experimentation. In addition, to confirm a role for  $H_2S$ , the  $H_2S$ -slow releasing molecule P-(4-methoxyphenyl)-p-4-morpholinylphosphino-dithioic acid morpholine salt (GYY4137; Sigma-Aldrich, UK) was used. GYY4137 (1 M stock) was dissolved in DMSO and stored at  $-80$  °C, on the day of experiments the stock was diluted to 100 mM in perfusate and used on the same day, the final concentration of DMSO in the bath did not exceed 0.001%, when higher GYY4137 concentrations were used a 20 mM stock was made fresh in PBS and used on the same day for these experiments.

## Results

To examine whether Kv2.1 could be regulated by  $H_2S$ , we firstly recorded whole-cell currents from HEK293 cells stably expressing recombinant Kv2.1, as previously described<sup>28</sup>. Bath application of the  $H_2S$  donor, NaHS (20  $\mu$ M–1 mM), inhibited currents flowing through Kv2.1 channels in a concentration-dependent manner (Fig. 1A,B,C). Currents were inhibited at all activating test potentials (Fig. 1B) and there was no significant effect of NaHS on whole-cell conductance (Fig. 1C), suggesting that inhibition of current amplitudes was not attributable to altered gating. Inhibition of Kv2.1 currents was largely irreversible upon washout (e.g. Fig. 1E;  $23.5 \pm 4.1\%$  recovery after 10 min,  $n = 12$ ). However, current amplitudes could be recovered to near pre-NaHS treatment levels by exposure to the reducing agent dithiothreitol (DTT, 1 mM; Fig. 1F,  $83.4 \pm 3.7\%$  recovery,  $n = 13$ ). Similar results were obtained using another  $H_2S$  donor molecule GYY4137 (Fig. 2). Kv2.1 currents at test potentials greater than +40 mV by 30  $\mu$ M GYY4137 (Fig. 2A,B), this concentration was determined following a dose-response relationship for the effects of the  $H_2S$  donor GYY4137 (Fig. 2D). Normalized current amplitudes was inhibited by  $40.1 \pm 8.2\%$ ,  $n = 15$ , measured at +50 mV and this inhibition was irreversible upon washout (Fig. 2C).

Reversal of  $H_2S$  inhibition of Kv2.1 by DTT suggested a possible involvement of redox regulation of the channel protein. Sesti and colleagues<sup>29</sup> have demonstrated that cysteine 73 is crucial to the response of this channel to oxidation, and so we generated a C73A mutant to explore the role of this residue in  $H_2S$  regulation. As exemplified in Fig. 3A, and quantified in Fig. 3B, NaHS was without effect on the C73A mutant, whilst wild-type channels, studied in parallel, were significantly inhibited. Kv2.1 protein has an array of modifiable cysteine residues, some of which are not sensitive to oxidative modification<sup>29</sup>. To determine a role for other cysteine residues in the observed NaHS effect, we generated several other mutant cell lines. C29A and C831A still provided functional channels however both cell lines were sensitive to inhibition following application of 250  $\mu$ M NaHS (C831A by  $20 \pm 2\%$  ( $n = 6$ ); C29A by  $26.4 \pm 4\%$  ( $n = 5$ ), (Fig. 3C,D).

Many of the diverse effects of  $H_2S$  in different systems arise due to specific, direct modulation of target proteins by S-sulphydration (i.e. the conversion of –SH groups in cysteine residues into –SSH groups). S-sulphydration is detectable via the modified biotin switch assay<sup>18</sup>, and this approach was taken with the recombinant Kv2.1 protein. As illustrated in Fig. 4A, NaHS did indeed S-sulphydrate recombinant Kv2.1, evident from 30 mins, suggesting that the mechanism of channel inhibition was due to direct protein modification (full blots can be found as Supplementary Figures S1, 2 online). This was supported by the observation that the C73A mutant form of the channel appeared resistant to this form of post-translational modification (Fig. 4A; full blots available as Supplementary Figure S3 online). To provide a level of quantification  $50.8 \pm 7.5\%$ , ( $n = 3$ ) of WT Kv2.1 channel protein (Fig. 4B) can be identified as S-sulphydrated after 2 h treatment with NaHS (250  $\mu$ M) following modified biotin switch assay (time dependence further explored in Supplementary Figure S4 online). The time discrepancies observed between functional and biochemical experimentation are likely to reflect technical limitations of single cell versus population studies. The combination of these methodologies has been extensively used when examining post-translational modifications of plasma membrane proteins.

Kv2.1 is widely expressed in the CNS, and its ability to control the firing pattern of hippocampal neurons in particular has been described in detail (reviewed in Ref.<sup>25</sup>). As with HEK293 cells, we employed whole-cell patch-clamp recordings to demonstrate that NaHS caused significant inhibition of  $K^+$  currents in hippocampal rat neurons (Fig. 5A,B), at all activating test potentials studied. As was the case for recombinant Kv2.1, NaHS-mediated inhibition of  $K^+$  current amplitudes in hippocampal neurons could be recovered by DTT (1 mM; Fig. 5C).

Numerous different voltage-gated  $K^+$  currents contribute to the whole-cell  $K^+$  current in these cells. We and others have previously demonstrated that the contribution to the whole-cell current by Kv2.1 can be determined by intracellular dialysis (via the patch pipette) of an anti-Kv2.1 antibody<sup>28,30</sup>. In agreement with our earlier studies, intracellular dialysis with this antibody reduced current amplitudes by around 50% (Fig. 5D). Subsequent exposures to NaHS (100  $\mu$ M) did not significantly reduce currents further (Fig. 5D), indicating that NaHS was selective in its ability to inhibit Kv2.1 despite the presence of other voltage-gated  $K^+$  channels in hippocampal neurons.

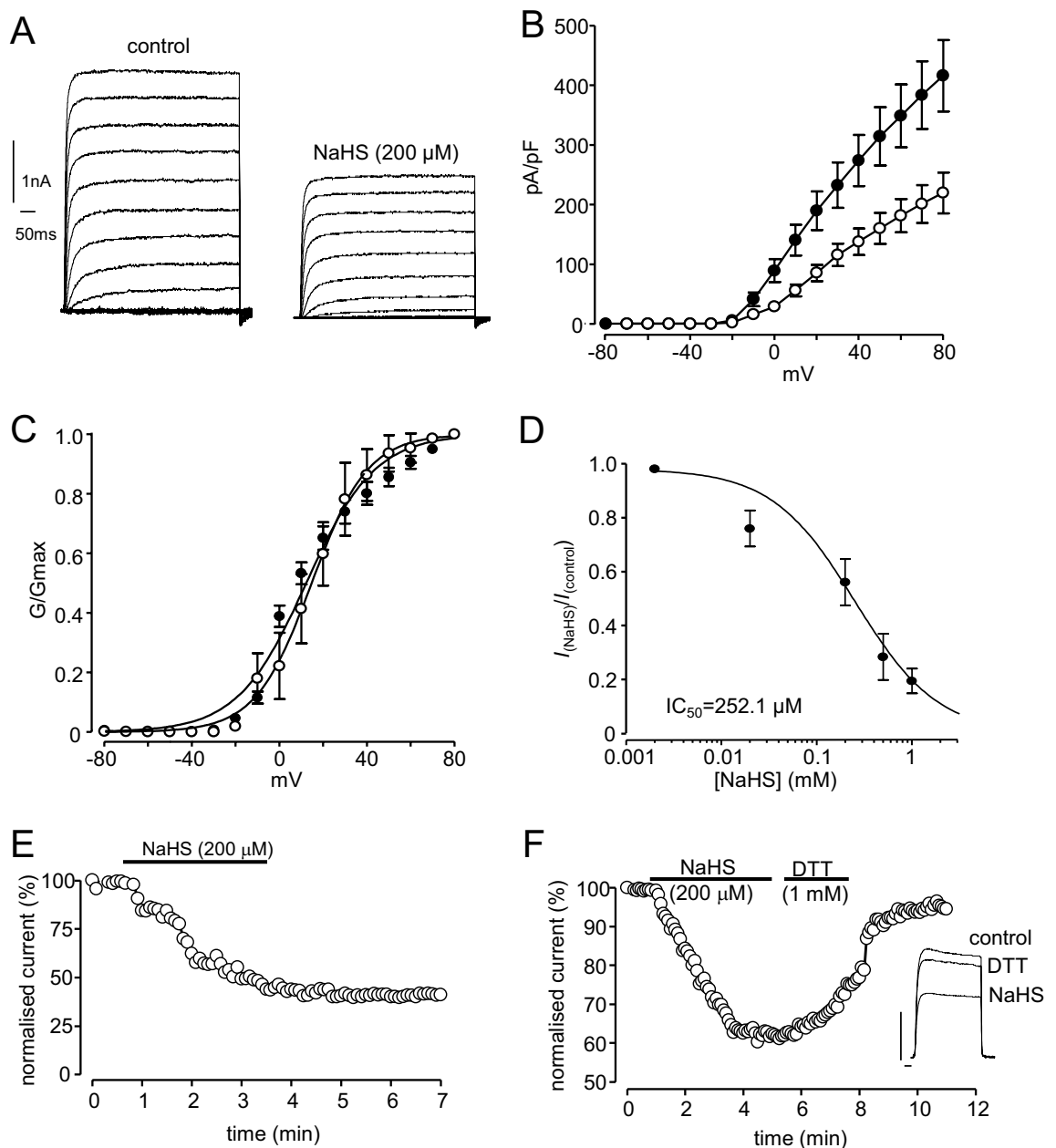


**Figure 1.** NaHS inhibits recombinant Kv2.1. (A) Families of currents evoked in a HEK293 cell stably expressing Kv2.1 before and during exposure to NaHS (200 μM). Currents were evoked by step-depolarizations, applied up to +80 mV in 10 mV increments from a holding potential of -70 mV. Scale bars apply to both families of currents. (B) Mean ( $\pm$  s.e.m.) current-density versus voltage relationships obtained in 17 cells before (solid circles) and during (open circles) exposure to NaHS (200 μM). (C) Mean ( $\pm$  s.e.m., each point taken from 5 to 7 cells) concentration-response relationship illustrating the effects of NaHS on Kv2.1. Inhibition was determined using currents evoked by step-depolarizations from -70 to +50 mV. (D) Plot of voltage-dependence of activation of Kv2.1 before (solid circles) and during (open circles) exposure to NaHS (200 μM). Data are means  $\pm$  s.e.m. Curves were obtained by fitting data to the sigmoidal Boltzmann function. (E) Example time-series plot illustrating normalized current amplitudes evoked by step-depolarizations from -70 to +50 mV in a Kv2.1-expressing HEK293 cell. For the period indicated by the horizontal bar, NaHS (200 μM) was applied via the perfusate. (F) as (E), except that, following washout of NaHS, the cell was exposed to dithiothreitol (DTT, 1 mM) for the period indicated by the second horizontal bar. Inset shows example currents under the conditions indicated (DTT applied after washout of NaHS). Scale bars: 2 nA (vertical) and 10 ms (horizontal).

Kv2.1 channel activity is a major determinant of hippocampal neuronal excitability, and can be dramatically modified, for example, by phosphorylation<sup>25,26</sup>. To investigate whether  $H_2S$  could alter hippocampal excitability, we employed current-clamp recordings. Application of NaHS caused a modest yet significant depolarization of



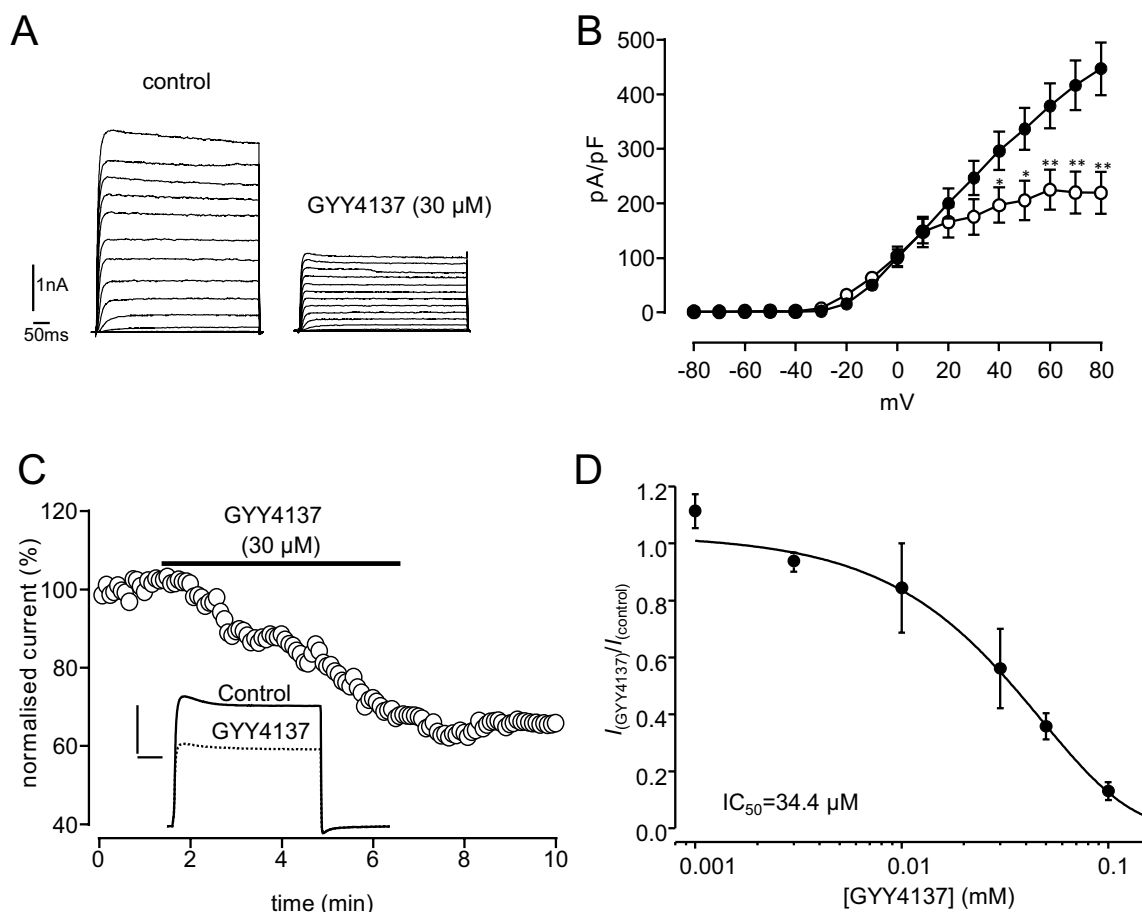


**Figure 2.** GYY4137 inhibits recombinant Kv2.1. (A) Families of currents evoked in a HEK293 cell stably expressing Kv2.1 before and during exposure to GYY4137 (30  $\mu$ M). Currents were evoked by step-depolarizations, applied up to +80 mV in 10 mV increments from a holding potential of -70 mV. Scale bars apply to both families of currents. (B) Mean ( $\pm$  s.e.m.) current-density versus voltage relationships obtained in 11 cells before (solid circles) and during (open circles) exposure to GYY4137 (30  $\mu$ M). Significance: \* $P$  < 0.05; \*\* $P$  < 0.01 as compared with controls. (C) Example time-series plot illustrating normalized current amplitudes evoked by step-depolarizations in a Kv2.1-expressing HEK293 cell. For the period indicated by the horizontal bar, GYY4137 (30  $\mu$ M) was applied via the perfusate, indicated by horizontal bar, followed by washout. Inset shows example currents under the different experimental conditions scale bars: 2 nA (vertical) and 10 ms (horizontal). (D) Mean ( $\pm$  s.e.m., each point taken from 3 to 5 cells) concentration-response relationship fitted to sigmoidal Boltzmann function illustrating the effects of GYY4137 on Kv2.1. Inhibition was determined using currents evoked by step-depolarizations from -70 to +50 mV.

cells ( $9.1 \pm 1.8$  mV,  $n = 6$ ,  $P < 0.01$ ), indicative of reported  $H_2S$  effects on TRP channels in dorsal root ganglion neurons<sup>31</sup>. This effect was compensated by current injection, in order to examine the effects of depolarizing current injections in cells with a standardised membrane potential of -70 mV (Fig. 5A,B). Square wave current injections evoked action potentials which increased in frequency with increasing current amplitude (Fig. 5A,B). In the presence of NaHS (200  $\mu$ M), action potential frequency was augmented, particularly following larger current injections, as anticipated when Kv2.1 channels participate in neuronal excitability.

## Discussion

Our study identifies  $H_2S$  as another important modulator of the voltage-gated  $K^+$  channel Kv2.1. This channel is highly expressed in the cortex and hippocampus where it is a major determinant of intrinsic neuronal excitability through a diverse complement of signalling cascades. High levels of constitutive phosphorylation determine the voltage-dependence of gating and location of Kv2.1, and both factors can influence neuronal excitability in a dynamic manner<sup>25, 32, 33</sup>. Activity-dependent, calcineurin-mediated dephosphorylation of Kv2.1 can suppress excitability<sup>33</sup>, and rapid rephosphorylation (e.g. via CDK5<sup>34</sup>) can restore excitability. However, this is dependent on the location of the phosphorylation site within the channel protein: for example, AMP-activated protein kinase-mediated phosphorylation at distinct residues (S440 and S537) can suppress excitability and exert hyperpolarizing shifts in the voltage-dependent activation, similar to calcineurin-mediated dephosphorylation of other residues<sup>27</sup>. In addition to alteration of gating via phosphorylation, Kv2.1 channel inhibition

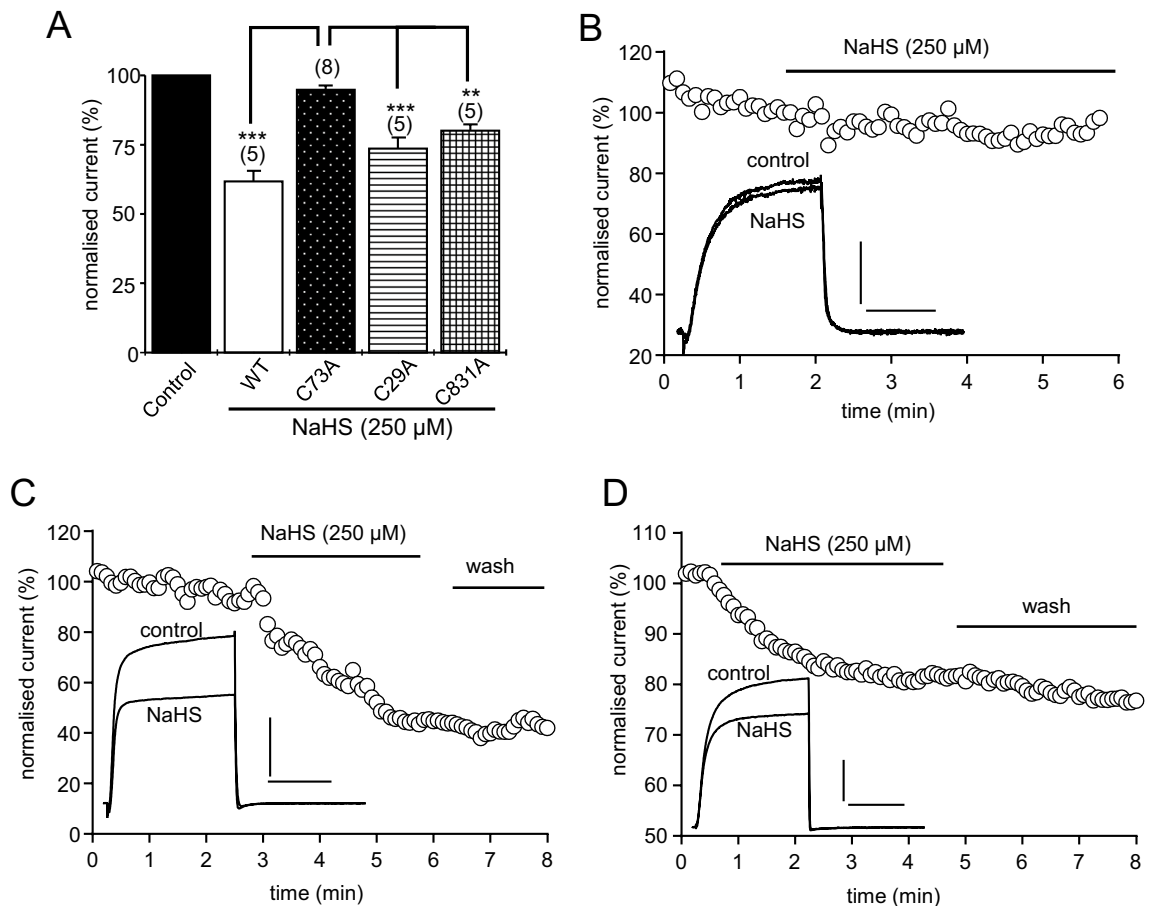


**Figure 3.**  $\text{H}_2\text{S}$  does not inhibit Kv2.1 C73A but inhibit other recombinant mutant forms. **(A)** Bar graph showing normalised mean ( $\pm$  s.e.m.) effect of NaHS in wild-type (WT), C73A, C29A and C831A mutants of Kv2.1, as indicated (\*\* indicates  $P < 0.01$  and \*\*\* indicates  $P < 0.001$  with the number of cells tested in parentheses). **(B)** Example time-series plot illustrating normalized current amplitudes evoked by step-depolarizations from  $-70$  to  $+50$  mV in a C73A Kv2.1-expressing HEK293 cell. For the period indicated by the horizontal bar, NaHS ( $250 \mu\text{M}$ ) was applied via the perfusate. Inset shows example currents before and during NaHS application, as indicated. **(C)** Example time-series plot as in **(B)** for C29A Kv2.1-expressing HEK293 cell. For the period indicated by the horizontal bar, NaHS ( $250 \mu\text{M}$ ) was applied via the perfusate, with irreversible effect upon washout for the time period indicated by the horizontal bar. Inset shows example currents before and during NaHS application for C29A, as indicated. **(D)** Same as in **(B)** and **(C)** except the example time-series plot illustrating a C831A Kv2.1-expressing HEK293 cell before and during application of NaHS ( $250 \mu\text{M}$ ) for the period indicated by the horizontal bar, as in **(C)** the effect was irreversible upon washout, indicated by the horizontal bar. Inset shows example currents before and during NaHS application for C831A. Scale bars:  $0.5$  nA (vertical) and  $50$  ms (horizontal).

(e.g. following antisense knockdown) also increases high frequency excitability<sup>35,36</sup>. The present study indicates that this phenomenon also occurs because of channel inhibition by  $\text{H}_2\text{S}$  (Fig. 3). Thus, using larger depolarizing current injections, action potential frequency was augmented by  $\text{H}_2\text{S}$ , suggesting that this gasotransmitter may influence excitability physiologically through modulation of Kv2.1 selectively. It remains to be determined if polysulfides mediated this inhibition as has been reported for Kv1.4 and Kv3.4<sup>23</sup>. This is likely to be mediated via S-sulphydration of the channel given our biochemical evidence. There are time discrepancies between the acute exposure in the functional recordings and the biochemical observations, but these are comparable to other reports of ion channel post-translational modification (see Ref.<sup>18</sup>). This likely reflects the number of S-sulphydrated channels required to produce a functional effect versus the amount of S-sulphydrated protein detected via our biochemical experimentation.

Such complex regulation of a single channel target suggests it is of fundamental importance to the excitability of neurons in which it is expressed, but the fact that it is also a target for modulation by gasotransmitters supports the belief that it has even greater physiological significance. While evidence exists that other Kv channels are modulated by  $\text{H}_2\text{S}$ , such as Kv7<sup>24,37,38</sup>, the neuronal localisation of these channels will ultimately determine their influence on action potential dynamics. For example, Kv7 activation via NaHS has been reported to suppress neuropathic pain<sup>24</sup>, indicative of a decrease in network excitability<sup>39</sup>. These studies have implicated the  $\text{H}_2\text{S}$  in the mechanisms of neuropathic pain mediated by the Kv7 family. This furthers the diversity of ion channels targeted



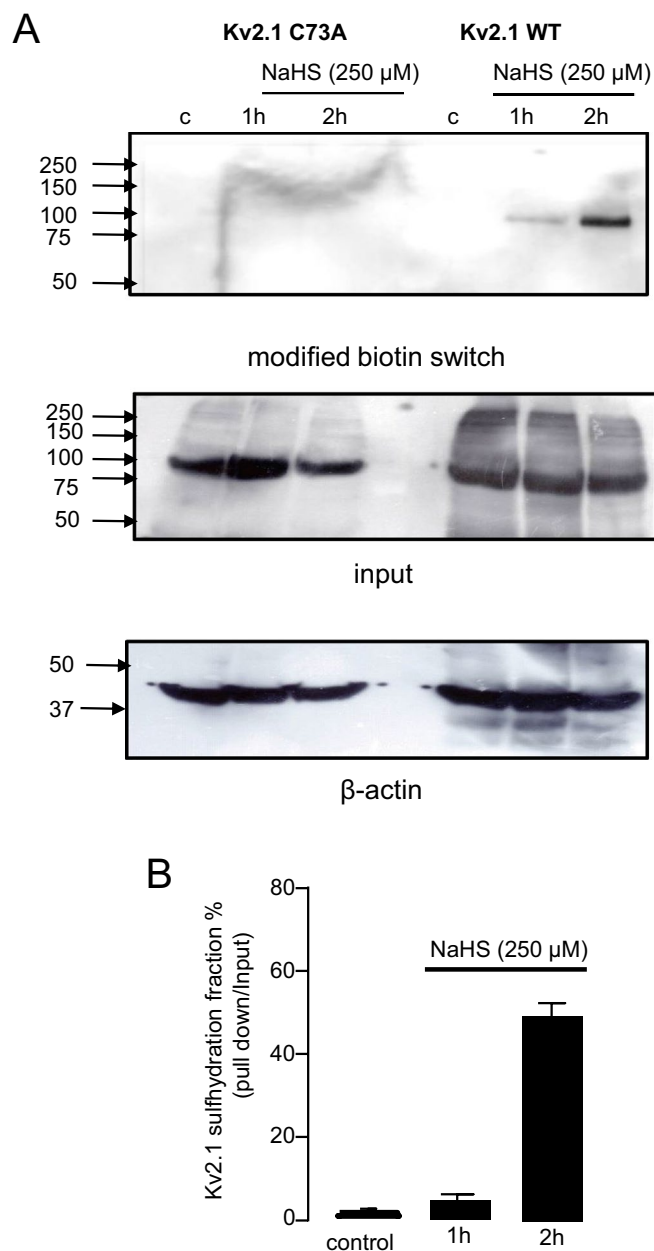
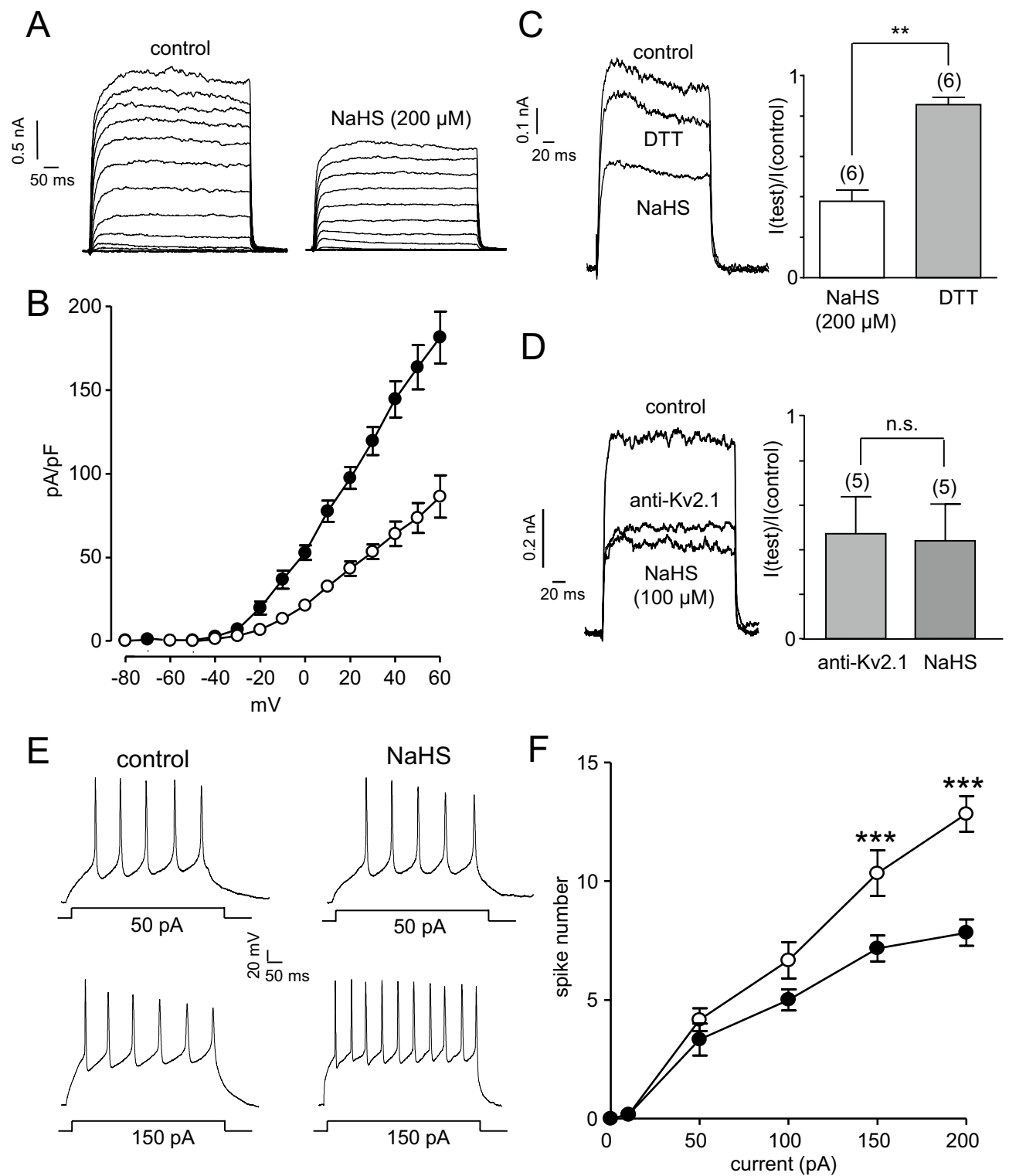


**Figure 4.** Kv2.1 sensitivity to NaHS is mediated by cysteine 73. **(A)** S-sulfhydration of WT but not C73A Kv2.1 by NaHS (250  $\mu$ M) in HEK293 cells as detected by western blot analysis of biotinylated proteins produced by the modified biotin switch assay (upper bands). Middle bands demonstrate Kv2.1 protein input. Lower bands shows the loading control  $\beta$ -actin. Representative of five experimental repeats. **(B)** % fraction of S-sulfhydrated Kv2.1 following modified biotin switch assay over a 2 h period.

by  $H_2S$  and also raises questions over selectivity<sup>20</sup>. With respect to the hippocampus, Kv7 channels has been localised to the axonal initial segment<sup>40</sup> in contrast Kv2.1 channels display a predominant somatodendritic loci<sup>41</sup>. Therefore, discrete localisation of Kv channels<sup>42,43</sup> may underpin the respective action of  $H_2S$  on neuronal output.

Kv2.1 has also been proposed to play a vital role in oxidative stress-induced apoptosis of central neurons: oxidants can initiate apoptosis in a  $Zn^{2+}$ -dependent manner which leads to co-ordinated, Src kinase-mediated phosphorylation of the channel protein at an N-terminal tyrosine (Y124) together with p38 MAPK-mediated phosphorylation at a C-terminal site (S800). This in turn leads to rapid channel insertion into the plasma membrane; the resultant loss of cytosolic  $K^+$  triggers caspase activation and apoptosis. The present study suggests  $H_2S$  may provide protection against oxidant-induced apoptosis via inhibition of Kv2.1. Indeed, we have previously shown that Kv2.1 is inhibited by carbon monoxide (CO), which is derived from heme oxygenases (HO-1 and HO-2). The inducible heme oxygenase, HO-1, is upregulated by numerous stress factors and its ability to provide protection against apoptosis in hippocampal neurons arises, at least in part, from the ability of its product, CO,



◀ **Figure 5.** NaHS inhibits Kv2.1 and augments action potential firing in rat hippocampal neurons. **(A)** Families of currents evoked in a rat hippocampal neuron before and during exposure to NaHS (200  $\mu$ M). Currents were evoked by step-depolarizations, applied up to +60 mV in 10 mV increments from a holding potential of -70 mV. Scale bars apply to both families of currents. **(B)** Mean ( $\pm$  s.e.m.) current-density versus voltage relationships obtained in 8 cells before (solid circles) and during (open circles) exposure to NaHS (200  $\mu$ M). **(C)** Left, example currents evoked in the same neuron before (control) and during exposure to NaHS (200  $\mu$ M), then during a subsequent exposure to DTT (1 mM) following washout of NaHS. Right, bar graph showing normalised mean ( $\pm$  s.e.m.) effect of NaHS and recovery of current amplitude by DTT. (\*\*Indicates  $P < 0.01$  with the number of cells tested in parentheses). **(D)** Left, example currents evoked in the same neuron immediately after obtaining the whole-cell configuration, after 10 min dialysis with an anti-Kv2.1 antibody, and then during a subsequent exposure to NaHS (100  $\mu$ M), as indicated. Right, bar graph showing normalised mean ( $\pm$  s.e.m.) effect of the anti-Kv2.1 antibody, and the effects of NaHS following a minimum of 10 min dialysis in these cells. (n.s. indicates  $P > 0.05$  with the number of cells employed indicated in parentheses). **(E)** Example voltage responses evoked by square wave depolarizing current injections (upper traces 50 pA, lower traces 150 pA) in hippocampal neurones perfused in the absence (left hand traces) or presence (right hand traces) of NaHS (200  $\mu$ M). Scale bars apply to all traces. **(F)** Mean ( $\pm$  s.e.m.) number of evoked action potentials measured in response to 500 ms depolarizing current injections of varying amplitude. Action potentials were measured in the absence (solid circles) or presence (open circles) of 200  $\mu$ M NaHS (\*\*\*indicates  $P < 0.005$ ,  $n = 6$  for all current steps).

to inhibit Kv2.1<sup>28</sup>. Interestingly, a similar Kv2.1-mediated protective mechanism may be active in some forms of cancer (in which resistance to apoptosis is a hallmark feature of the disease<sup>44</sup>) where HO-1 expression is constitutively high<sup>45</sup>.

Interestingly, research indicates that oxidative stress can modify Kv2.1 channels via a novel means, causing their oligomerization through formation of disulfide bridges with adjacent channel proteins. This in turn leads to channel clustering and promotion of apoptosis<sup>29</sup>, and it was proposed that this is an important aspect of both normal, age-related loss of neuronal function which is exacerbated in Alzheimer's disease<sup>29</sup>. Animal studies also highlight modulation of the Kv2.1 protein function, to increase hippocampal neuronal excitability, in the 3xTg-AD model of Alzheimer's disease<sup>46</sup>. In this regard, channel inhibition by H<sub>2</sub>S may be of particular importance: the modified biotin switch assay revealed that H<sub>2</sub>S caused S-sulfhydration of the channel protein (Fig. 2C), and this has been proposed to provide protection of vulnerable cysteine residues against oxidation<sup>1</sup>. This could have implications for cognitive decline and supports the use of H<sub>2</sub>S donors to modulate Alzheimer's pathology<sup>47–49</sup> however further consideration of the temporal profile of pathology alongside H<sub>2</sub>S administration is required.

In summary, we have shown that H<sub>2</sub>S inhibits both recombinant and native Kv2.1 and propose that this occurs via S-sulfhydration of the channel protein. This occurred in a concentration dependent manner; however, we cannot rule out the interactions of other proposed S-sulfhydrated molecular targets on our neuronal observations. However, consistent with the known physiological role of Kv2.1, we show that H<sub>2</sub>S-mediated inhibition contributes to augmentation of higher rates of evoked action potential frequencies with the Kv2.1 protein acting as a molecular rheostat<sup>50</sup>. This has implications for pathological conditions where (i) H<sub>2</sub>S production is altered (e.g. dementia<sup>51</sup>) or (ii) where the Kv2.1 protein has been oxidised at C73 (e.g. ageing<sup>29</sup>). Future studies will determine whether S-sulfhydration of Kv2.1 will provide protection against apoptosis arising from oxidative stress, for example, because of aging or neurodegenerative diseases.

Received: 20 June 2019; Accepted: 31 March 2021

Published online: 14 April 2021

## References

1. Paul, B. D. & Snyder, S. H. H<sub>2</sub>S signalling through protein sulfhydration and beyond. *Nat. Rev. Mol. Cell Biol.* **13**, 499–507 (2012).
2. Wang, R. Physiological implications of hydrogen sulfide: a Whiff exploration that blossomed. *Physiol. Rev.* **92**, 791–896 (2012).
3. Kimura, H., Shibuya, N. & Kimura, Y. Hydrogen sulfide is a signaling molecule and a cytoprotectant. *Antioxid. Redox Signal.* **17**, 45–57 (2012).
4. Shibuya, N., Mikami, Y., Kimura, Y., Nagahara, N. & Kimura, H. Vascular endothelium expresses 3-mercaptopyruvate sulfurtransferase and produces hydrogen sulfide. *J. Biochem.* **146**, 623–626 (2009).
5. Shibuya, N. *et al.* 3-Mercaptopyruvate sulfurtransferase produces hydrogen sulfide and bound sulfane sulfur in the brain. *Antioxid. Redox Signal.* **11**, 703–714 (2009).
6. Ishigami, M. *et al.* A source of hydrogen sulfide and a mechanism of its release in the brain. *Antioxid. Redox Signal.* **11**, 205–214 (2009).
7. Abe, K. & Kimura, H. The possible role of hydrogen sulfide as an endogenous neuromodulator. *J. Neurosci.* **16**, 1066–1071 (1996).
8. Kimura, H. Hydrogen sulfide induces cyclic AMP and modulates the NMDA receptor. *Biochem. Biophys. Res. Commun.* **267**, 129–133 (2000).
9. Olson, K. R., DeLeon, E. R. & Liu, F. Controversies and conundrums in hydrogen sulfide biology. *Nitric Oxide Biol. Chem.* **41**, 11–26 (2014).
10. Olson, K. R. A practical look at the chemistry and biology of hydrogen sulfide. *Antioxid. Redox Signal.* **17**, 32–44 (2012).
11. Wedmann, R. *et al.* Working with 'H<sub>2</sub>S': facts and apparent artifacts. *Nitric Oxide Biol. Chem.* **41**, 85–96 (2014).
12. Jiang, J. *et al.* Hydrogen sulphide—mechanisms of toxicity and development of an antidote. *Sci. Rep.* **6**, 1–10 (2016).
13. Reiffenstein, R. J., Hulbert, W. C. & Roth, S. H. Toxicology of hydrogen sulfide. *Annu. Rev. Pharmacol. Toxicol.* **32**, 109–134 (1992).
14. Kimura, Y. *et al.* Polysulfides are possible H<sub>2</sub>S-derived signaling molecules in rat brain. *FASEB J.* **27**, 2451–2457 (2013).
15. Kimura, H. Signalling by hydrogen sulfide and polysulfides via protein S-sulfuration. *Br. J. Pharmacol.* <https://doi.org/10.1111/bph.14579> (2019).

16. Nagai, Y., Tsugane, M., Oka, J. I. & Kimura, H. Hydrogen sulfide induces calcium waves in astrocytes. *FASEB J.* **18**, 557–559 (2004).
17. Kimura, Y. & Kimura, H. Hydrogen sulfide protects neurons from oxidative stress. *FASEB J.* **18**, 1165–1167 (2004).
18. Mustafa, A. K. *et al.* H<sub>2</sub>S signals through protein S-sulfhydration. *Sci. Signal.* **2**, ra72 (2009).
19. Sen, N. & Snyder, S. H. Protein modifications involved in neurotransmitter and gasotransmitter signaling. *Trends Neurosci.* **33**, 493–502 (2010).
20. Peers, C., Bauer, C. C., Boyle, J. P., Scragg, J. L. & Dallas, M. L. Modulation of ion channels by hydrogen sulfide. *Antioxid. Redox Signal.* **17**, 95–105 (2012).
21. Mustafa, A. K. *et al.* Hydrogen sulfide as endothelium-derived hyperpolarizing factor sulfhydrates potassium channels. *Circ. Res.* **109**, 1259–1268 (2011).
22. Jan, L. Y. & Jan, Y. N. Voltage-gated potassium channels and the diversity of electrical signalling. *J. Physiol.* **590**, 2591–2599 (2012).
23. Yang, K. *et al.* Modulation of K<sup>+</sup> channel N-type inactivation by sulfhydration through hydrogen sulfide and polysulfides. *Pflugers Arch.* **471**, 557–571 (2019).
24. Di Cesare Mannelli, L. *et al.* Effects of natural and synthetic isothiocyanate-based H<sub>2</sub>S-releasers against chemotherapy-induced neuropathic pain: role of Kv7 potassium channels. *Neuropharmacology* **121**, 49–59 (2017).
25. Mohapatra, D. P. *et al.* Regulation of intrinsic excitability in hippocampal neurons by activity-dependent modulation of the KV2.1 potassium channel. *Channels* **3**, 46–56 (2009).
26. Park, K.-S., Mohapatra, D. P., Misonou, H. & Trimmer, J. S. Graded regulation of the Kv2.1 potassium channel by variable phosphorylation. *Science* **313**, 976–9 (2006).
27. Ikematsu, N. *et al.* Phosphorylation of the voltage-gated potassium channel Kv2.1 by AMP-activated protein kinase regulates membrane excitability. *Proc. Natl. Acad. Sci.* **108**, 18132–18137 (2011).
28. Dallas, M. L. *et al.* Carbon monoxide protects against oxidant-induced apoptosis via inhibition of Kv2.1. *FASEB J.* **25**, 1519–1530 (2011).
29. Cotella, D. *et al.* Toxic role of K<sup>+</sup> channel oxidation in mammalian brain. *J. Neurosci.* **32**, 4133–4144 (2012).
30. Murakoshi, H. & Trimmer, J. S. Identification of the Kv2.1 K<sup>+</sup> channel as a major component of the delayed rectifier K<sup>+</sup> current in rat hippocampal neurons. *J. Neurosci.* **19**, 1728–35 (1999).
31. Andersson, D. A., Gentry, C. & Bevan, S. TRPA1 has a key role in the somatic pro-nociceptive actions of hydrogen sulfide. *PLoS ONE* **7**, e46917 (2012).
32. Misonou, H. *et al.* Regulation of ion channel localization and phosphorylation by neuronal activity. *Nat. Neurosci.* **7**, 711–718 (2004).
33. Misonou, H. *et al.* Bidirectional activity-dependent regulation of neuronal ion channel phosphorylation. *J. Neurosci.* **26**, 13505–13514 (2006).
34. Cerda, O. & Trimmer, J. S. Activity-dependent phosphorylation of neuronal Kv2.1 potassium channels by CDK5. *J. Biol. Chem.* **286**, 28738–48 (2011).
35. Du, J., Haak, L. L., Phillips-Tansey, E., Russell, J. T. & McBain, C. J. Frequency-dependent regulation of rat hippocampal somatodendritic excitability by the K<sup>+</sup> channel subunit Kv2.1. *J. Physiol.* **522**, 19–31 (2000).
36. Misonou, H., Mohapatra, D. P. & Trimmer, J. S. Kv2.1: A voltage-gated K<sup>+</sup> channel critical to dynamic control of neuronal excitability. *Neurotoxicology* **26**, 743–752 (2005).
37. Lucarini, E. *et al.* Effect of glucoraphanin and sulforaphane against chemotherapy-induced neuropathic pain: Kv7 potassium channels modulation by H<sub>2</sub>S release in vivo. *Phyther. Res.* **32**, 2226–2234 (2018).
38. Hedegaard, E. R. *et al.* Involvement of potassium channels and calcium-independent mechanisms in hydrogen sulfide-induced relaxation of rat mesenteric small arteries. *J. Pharmacol. Exp. Ther.* **356**, 53–63 (2016).
39. Sittl, R., Carr, R. W., Fleckenstein, J. & Grafe, P. Enhancement of axonal potassium conductance reduces nerve hyperexcitability in an in vitro model of oxaliplatin-induced acute neuropathy. *Neurotoxicology* **31**, 694–700 (2010).
40. Shah, M. M., Migliore, M., Valencia, I., Cooper, E. C. & Brown, D. A. Functional significance of axonal Kv7 channels in hippocampal pyramidal neurons. *Proc. Natl. Acad. Sci. U. S. A.* **105**, 7869–7874 (2008).
41. Trimmer, J. S. Immunological identification and characterization of a delayed rectifier K<sup>+</sup> channel polypeptide in rat brain. *Proc. Natl. Acad. Sci. U. S. A.* **88**, 10764–10768 (1991).
42. Trimmer, J. S. & Rhodes, K. J. Localization of voltage-gated ion channels in mammalian brain. *Annu. Rev. Physiol.* **66**, 477–519 (2004).
43. Vacher, H., Mohapatra, D. P. & Trimmer, J. S. Localization and targeting of voltage-dependent ion channels in mammalian central neurons. *Physiol. Rev.* **88**, 1407–1447 (2008).
44. Hanahan, D. & Weinberg, R. A. Hallmarks of cancer: the next generation. *Cell* **144**, 646–674 (2011).
45. Al-Owais, M. M. A. *et al.* Carbon monoxide mediates the anti-apoptotic effects of heme oxygenase-1 in medulloblastoma DAOY cells via K<sup>+</sup> channel inhibition. *J. Biol. Chem.* **287**, 24754–24764 (2012).
46. Frazzini, V. *et al.* Altered Kv2.1 functioning promotes increased excitability in hippocampal neurons of an Alzheimer's disease mouse model. *Cell Death Dis.* **7**, e2100 (2016).
47. Xuan, A. *et al.* Hydrogen sulfide attenuates spatial memory impairment and hippocampal neuroinflammation in beta-amyloid rat model of Alzheimer's disease. *J. Neuroinflamm.* **9**, 687 (2012).
48. Giuliani, D. *et al.* Hydrogen sulfide slows down progression of experimental Alzheimer's disease by targeting multiple pathophysiological mechanisms. *Neurobiol. Learn. Mem.* **104**, 82–91 (2013).
49. Vandini, E. *et al.* Mechanisms of hydrogen sulfide against the progression of severe Alzheimer's disease in transgenic mice at different ages. *Pharmacology* **103**, 93–100 (2019).
50. Romer, S. H., Deardorff, A. S. & Fyfe, R. E. W. A molecular rheostat: Kv2.1 currents maintain or suppress repetitive firing in motoneurons. *J. Physiol.* **597**, 3769–3786 (2019).
51. Kamat, P. K., Kyles, P., Kalani, A. & Tyagi, N. Hydrogen sulfide ameliorates homocysteine-induced Alzheimer's disease-like pathology, blood-brain barrier disruption, and synaptic disorder. *Mol. Neurobiol.* **53**, 2451–2467 (2016).

## Acknowledgements

This work was supported by a fellowship award from Alzheimer's Research UK (MLD) (Garnt No. ART-PSRF2011-1), Royal Society Research Grant Award (MLD) (Grant No. RG120400) and a Heart Research UK Grant (MMA) (Grant No. RG.IMSB.114615). We are extremely grateful to Professor Solomon H. Snyder (Johns Hopkins University) for valuable discussions during this study.

## Author contributions

M.L.D. and C.P. conceived the experiment(s), M.L.D., M.M.A., N.T.H., J.P.B., H.H.J.-G., M.S.V. conducted the experiment(s), J.L.S., D.S., provided experimental resources, M.L.D., M.M.A., N.T.H., analysed the results. All authors commented on the manuscript.

### Competing interests

The authors declare no competing interests.

### Additional information

**Supplementary information** The online version contains supplementary material available at <https://doi.org/10.1038/s41598-021-87646-5>.

**Correspondence** and requests for materials should be addressed to M.L.D. or M.M.A.-O.

**Reprints and permissions information** is available at [www.nature.com/reprints](http://www.nature.com/reprints).

**Publisher's note** Springer Nature remains neutral with regard to jurisdictional claims in published maps and institutional affiliations.



**Open Access** This article is licensed under a Creative Commons Attribution 4.0 International License, which permits use, sharing, adaptation, distribution and reproduction in any medium or format, as long as you give appropriate credit to the original author(s) and the source, provide a link to the Creative Commons licence, and indicate if changes were made. The images or other third party material in this article are included in the article's Creative Commons licence, unless indicated otherwise in a credit line to the material. If material is not included in the article's Creative Commons licence and your intended use is not permitted by statutory regulation or exceeds the permitted use, you will need to obtain permission directly from the copyright holder. To view a copy of this licence, visit <http://creativecommons.org/licenses/by/4.0/>.

© The Author(s) 2021